Transition from Nanopores to Nanotubes: Self-Ordered Anodic Oxide Structures on Titanium−Aluminides

Steffen Berger, Hiroaki Tsuchiya, and Patrik Schmuki*

Department of Materials Science, WW4-LKO, University of Erlangen-Nuremberg, Martensstrasse 7, D-91058 Erlangen, Germany

Received February 9, 2008
Revised Manuscript Received March 19, 2008

Self-ordering effects in anodic oxides on refractory metals are observed in two distinct morphologies: (i) highly ordered parallely aligned porous oxide structures and (ii) ordered arrays of oxide nanotubes. The most prominent example showing a self-ordered nanoporous oxide morphology is aluminum. Since Masuda et al.[1] reported the formation of highly ordered porous aluminum oxide layers in 1995, anodic self-ordering of aluminum oxide has become a topic of intense activity in several fields of research and technology.[1–14] Routes for fabrication are in most cases based on a simple but highly optimized anodization process of a pure Al metal sheet in a suitable acidic electrolyte[1–7] or using electrolytes with a small amount of fluoride additions[15,16] (see also Supporting Information S1). Fluoride containing electrolytes were also used to grow ordered porous oxides on W,[17] Ta,[18] and Nb.[19] In contrast to these metals, various other refractory metals such as Ti,[20,21] Zr,[22] and Hf[23] grow in fluoride containing electrolytes a tubular morphology that can be arranged in a highly ordered array pattern. The most prominent example for this morphology is titanium. This system is currently extensively investigated due to numerous potential fields of application. Ordered TiO_2 nanotube arrays have for example been explored in catalyst systems,[24–26] in solar energy conversion,[27,28] in sensors[29] in wettability tuning of surfaces,[30,31] in electrochromic devices,[32–34] and in biomedicine.[35,36] Due to the fundamentally different oxide morphologies that grow on Al and Ti it is highly interesting to study the behavior of various composition TiAl alloys anodized in a fluoride containing electrolyte and to evaluate the critical conditions for a transition from one morphology to the another. A second point of interest is the length scale of the self-organization process as the ordered oxide structures on Al and Ti are anodization voltage controlled[37,38] but the absolute self-ordering length is strongly different for the two substrates.

In the present work we investigate self-ordered oxide growth on Al, $TiAl_3$, TiAl, Ti_3Al, and Ti. This specific set of intermetallic compounds offers the possibility of a detailed investigation of the influence of the increasing titanium content on the key features of anodic oxide nanostructures. Except for scientific reasons, the ability to form highly self-ordered nanostructured oxide coatings on these intermetallic phases bears significant technological impact as in many cases these intermetallic compounds are used as a basis for numerous high performance titanium alloys. (TiAl alloys feature a high strength to density ratio and a high toughness which makes them suitable as a lightweight material in aircraft engineering or for medical applications[39]). In order to achieve self-ordered oxide features we use a fluoride based

* Corresponding author. E-mail: schmuki@ww.uni-erlangen.de. Tel.: +49-9131-852-7575.

(1) Masuda, H.; Fukuda, K. *Science* **1995**, *268*, 1466.
(2) Masuda, H.; Hasegwa, K.; Ono, S. *J. Electrochem. Soc.* **1997**, *144*, L127.
(3) Masuda, H.; Yada, K.; Osaka, A. *Jpn. J. Appl. Phys.* **1998**, *37*, L1340.
(4) Martin, C. R. *Science* **1994**, *266*, 1961.
(5) Li, A.-P.; Müller, F.; Birner, A.; Nielsch, K.; Gösele, U. *Adv. Mater.* **1999**, *11* (6), 483.
(6) Chu, S.-Z.; Wada, K.; Inoue, S.; Isogai, M.; Yasumori, A. *Adv. Mater.* **2005**, *17*, 2115.
(7) Lee, W.; Ji, R.; Goesele, G.; Nielsch, K. *Nat. Mater.* **2006**, *5*, 741.
(8) Masuda, H.; Satoh, M. *Jpn. J. Appl. Phys.* **1996**, *35*, L126.
(9) Martin, C. R. *Chem. Mater.* **1996**, *8*, 1739.
(10) Cheng, G.; Moskovits, M. *Adv. Mater.* **2002**, *14*, 1567.
(11) Wu, Y.; Livneh, T.; Zhang, Y. Z.; Cheng, G.; Wang, J.; Tnag, J.; Moskovits, M.; Stucky, G. D *Nano Lett.* **2004**, *4* (12), 2337.
(12) Wu, Y.; Cheng, G.; Katsov, K.; Sides, S. W.; Wang, J.; Tang, J.; Fredrickson, G. H.; Moskovits, M.; Stucky, G. D. *Nat. Mater.* **2004**, *3*, 816.
(13) Hou, S.; Wang, J.; Martin, C. R. *Nano Lett.* **2005**, *5* (2), 231.
(14) Drury, A.; Chaure, S.; Kroll, M.; Nicolosi, V.; Chaure, N.; Blau, W. J. *Chem. Mater.* **2007**, *19*, 4252.
(15) Tsuchiya, H.; Berger, S.; Macak, J. M.; Munoz, A. G.; Schmuki, P. *Electrochem. Commun.* **2007**, *9* (4), 545.
(16) Tsuchiya, H.; Berger, S.; Macak, J. M.; Ghicov, A.; Schmuki, P. *Electrochem. Commun.* **2007**, *9* (9), 2397.
(17) Tsuchiya, H.; Macak, J. M.; Sieber, I.; Taveira, L.; Ghicov, A.; Sirotna, K.; Schmuki, P. *Electrochem. Commun.* **2005**, *7*, 295.
(18) Sieber, I.; Kannan, B.; Schmuki, P. *Electrochem. Solid-State Lett.* **2005**, *8*, J10.
(19) Sieber, I.; Hildebrand, H.; Friedrich, A.; Schmuki, P. *Electrochem. Commun.* **2005**, *7*, 97.
(20) Macak, J. M.; Tsuchiya, H.; Schmuki, P. *Angew. Chem., Int. Ed.* **2005**, *44*, 2100.
(21) Macak, J. M.; Tsuchiya, H.; Ghicov, A.; Yasuda, K.; Hahn, R.; Bauer, S.; Schmuki, P. *Curr. Opin. Sol. State Mater. Sci.*, **2008**, doi:10.1016/j.cossms.2007.08.004.
(22) Tsuchiya, H.; Schmuki, P. *Electrochem. Commun.* **2004**, *6*, 1131.
(23) Tsuchiya, H.; Schmuki, P. *Electrochem. Commun.* **2005**, *7*, 49.
(24) Macak, J. M.; Barczuk, J. P.; Tsuchiya, H.; Nowakowska, M. Z.; Ghicov, A.; Chojak, M.; Bauer, S.; Virtanen, S.; Kulesza, P. J.; Schmuki, P. *Electrochem. Commun.* **2005**, *7* (12), 1417.
(25) Macak, J. M.; Zlamal, M.; Krysa, J.; Schmuki, P. *Small* **2007**, *3* (2), 300.
(26) Macak, J. M.; Schmidt-Stein, F.; Schmuki, P. *Electrochem. Commun.* **2007**, *9* (7), 1783.
(27) Macak, J. M.; Tsuchiya, H.; Ghicov, A.; Schmuki, P. *Electrochem. Commun.* **2006**, *7*, 1133.
(28) Hahn, R. *Phys. Status Solidi RRL* **2007**, *1* (4), 135.
(29) Varghese, O. K.; Gong, D.; Paulose, M.; Ong, K. G.; Grimes, C. A. *Sens. Actuators, B-Chem.* **2003**, *93*, 338.
(30) Balaur, E.; Macak, J. M.; Tsuchiya, H.; Schmuki, P. *J. Mater. Chem.* **2005**, *15*, 4488.
(31) Balaur, E.; Macak, J. M.; Taveira, L.; Schmuki, P. *Electrochem. Commun.* **2005**, *7*, 1066.
(32) Ghicov, A.; Schmidt, B.; Kunze, J.; Schmuki, P. *Chem. Phys. Lett.* **2007**, *433* (4−6), 323.
(33) Ghicov, A.; Tsuchiya, H.; Hahn, R.; Macak, J. M.; Munoz, A. G.; Schmuki, P. *Electrochem. Commun.* **2005**, *8*, 528.
(34) Hahn, R.; Ghicov, A.; Tsuchiya, H.; Macak, J. M.; Munoz, A. G.; Schmuki, P. *Phys. Status Solidi A* **2007**, *204* (5), 1281.
(35) Tsuchiya, H.; Macak, J. M.; Müller, L.; Kunze, J.; Müller, F.; Greil, P.; Virtanen, S.; Schmuki, P. *J. Biomed. Mater. Res., Part A* **2006**, *77A*, 534.
(36) Park, J.; Bauer, S.; Mark, K. v. d.; Schmuki, P. *Nano Lett.* **2007**, *7* (6), 1686.
(37) Ono, S.; Masuko, N. *Surf. Coat. Technol.* **2003**, *169−170*, 139.
(38) Bauer, S.; Kleber, S.; Schmuki, P. *Electrochem. Commun.* **2006**, *8*, 1321.
(39) Leyens C., Peters M. *Titanium and Titanium Alloys*; Wiley-VCH: Weinheim, 2003.

10.1021/cm8004024 CCC: $40.75
Published on Web 05/06/2008

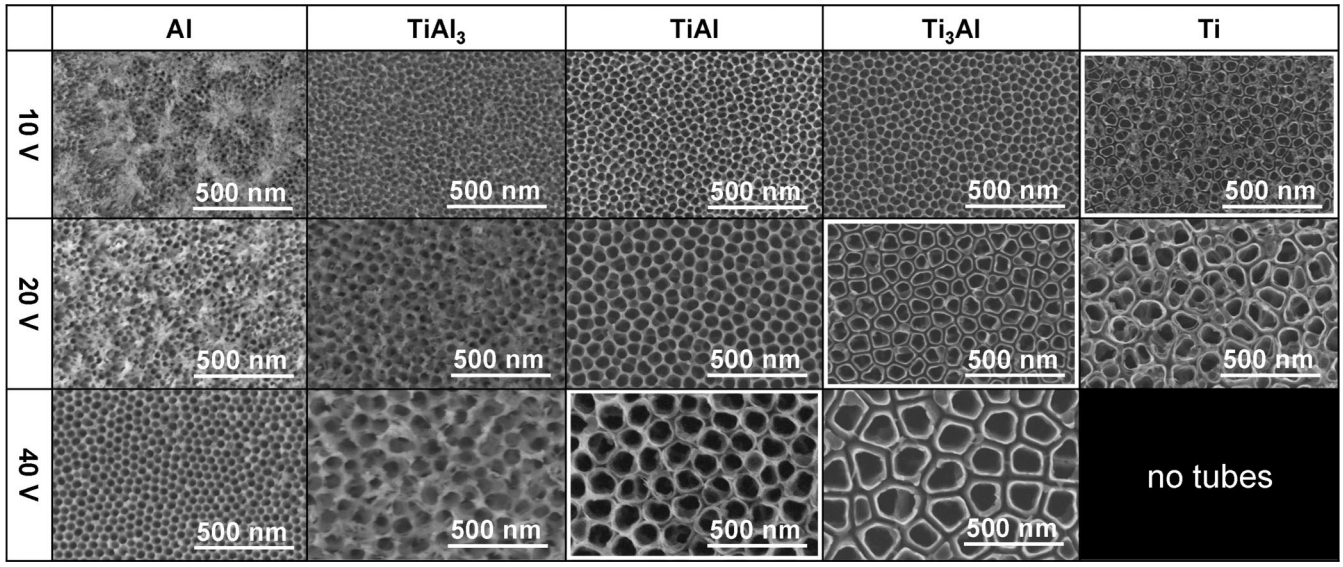

Figure 1. Top view SEM images of oxide-layers on Al, $TiAl_3$, TiAl, Ti_3Al, and Ti grown in 1 M H_2SO_4 containing 0.15 wt % HF at potentials of 10, 20, and 40 V. Transition from porous to tubular structure is highlighted.

electrolyte that has successfully been applied previously to create self-ordered nanoporous oxide structures on Al[2,37] and nanotubular oxide structures on Ti.[18] Details on the experimental procedure are given in the Supporting Information.

Figure 1 shows an overview of the morphologies formed on the different alloys at different anodization voltages. It is clear that self-organized oxide layers can be formed over a wide potential range. As a measure for the length scale of ordering one may use the interpore distance. On aluminum very regular porous structure can be observed, consisting of hexagonal nanopores with the average interpore distance increasing from 30 nm at 10 V to 55 nm at 40 V. While at lower potentials the pores are partially covered by bundles of oxide needles due to slow inhomogeneous chemical etching of the pore walls during extended anodization in fluoride containing electrolytes[15] this surface decoration is dissolved at higher voltages, allowing one to see the regular porous geometry underneath.

With increasing Ti content in the intermetallic compound, clearly the interpore distance in the formed porous oxide structures increases and under certain conditions (alloy composition and applied voltage) the porous features separate into an organized tubular structure. The higher the Ti content in the base material the more the transition is shifted to lower voltages. Figure 2a gives the critical voltage for tube separation as a function of the alloy composition.

On pure titanium, separated, self-organized nanotubes are already grown at 1 V.[38] At potentials higher than ~25 V no tubular layers can be grown anymore due to dielectric breakdown events. The latter determines the upper end of the potential window where self-ordered tube formation is possible. Obviously this window is smaller for Ti than for the investigated alloys. The results clearly demonstrate how the morphology of anodized layers is affected by the electrochemical conditions, in terms of anodization voltage and the alloy composition. Also the thickness of the oxide layers grown on the different materials drops by a factor of 40 from the pure aluminum (40 μm) to the $TiAl_3$ (960 nm), and for Ti_3Al only a thickness of approximately 290 nm is reached (see Supporting Information, Figure S2) due to the lower current densities that are obtained with increasing Ti

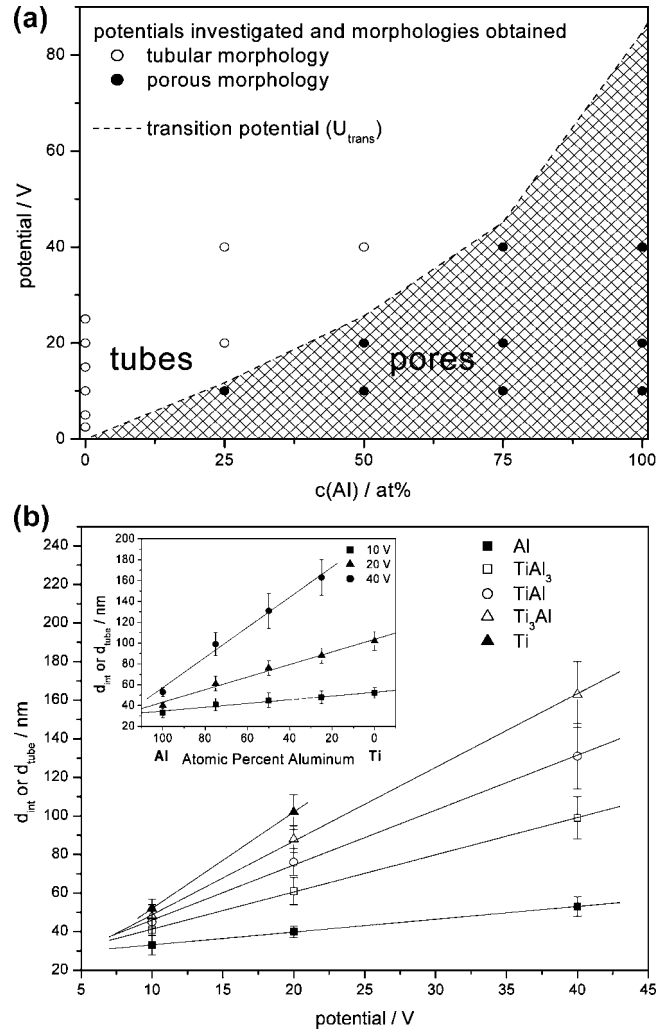

Figure 2. a. Dependence of the alloy composition on the morphology transition potential (pores to tubes). b. Dependence of the interpore distance (d_{int}) and the outer tube diameter (d_{tube}) on the anodizing potential. In the inset picture d_{int} and d_{tube} of the layers are plotted against the titanium content for different voltages.

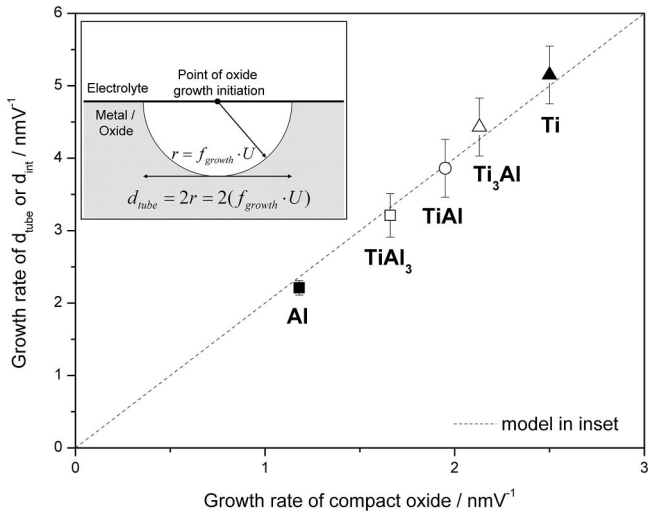

Figure 3. Correlation between literature data for the growth rates of compact oxide layer (growth factor) and the observed interpore distance (d_{int}) or the outer tube diameter (d_{tube}) within this work. The dashed line marks the relationship expected from the model depicted in the inset.

content (see Supporting Information, Figure S3). Interestingly, tubes grown on Ti_3Al were smooth-walled while the tubes grown on pure titanium showed the typical ripple structure on their side walls. This may possibly be explained in terms of current burning[40] or a pH fluctuation model.[41] In order to evaluate the influence of the alloying element content on the length scale of self-ordering, the interpore distance (d_{int}), or the tube diameter (d_{tube}) is plotted versus the different anodization potentials (Figure 2b) and versus the alloy composition (inset of Figure 2b), as shown.

The data show that the interpore distance or tube diameter depends linearly on the Ti content and the anodization potential. A model to explain the length scale of the self-organization which was recently postulated by Yasuda et al.[42] was applied to the data obtained in this work. The original data of Yasuda were found to hold for pure Ti and pure Al but has showed strong deviations for other metals. The results for the alloys used here are given in Figure 3, and a remarkably good agreement is found holding over the entire composition range and independent of the morphology (tubular or porous). The model essentially implies that the tube diameter (d_{tube}) of ordered nanotubular layers on various valve metals essentially depends on the oxide growth factor f_{growth}[42] (f_{growth} represents the proportionality between thickness t and anodization voltage U for the growth of compact valve metal oxide layers [$t = f_{growth}U$]). The concept assumes that anodic oxide growth starts from a point source on the metal surface, for example, at a local oxide breakdown site. From this point source immediately oxide growth would take place in all directions leading to a hemispherical oxide structure with a radius $r = f_{growth}U$, and this is schematically depicted in the inset of Figure 3. Repeated breakdown at the bottom of the pores would then lead to an oxide tube diameter d_{tube} of $d = 2r = 2f_{growth}U$. The fact that not only the dimensions of the self-ordered structures but also their nature (tubular or porous) are affected by the anodizing potential as well as by the chemical compositions of the alloys may be inherent to the oxide growth factor. The oxide growth factor is to a certain degree dependent on the volume expansion during oxide growth, the Pillings−Bedworth ratio,[43–46] and may be related to stress generated during oxide formation. Therefore the dependence of the transition potential U_{trans} on the alloy composition indicates a connection not only to the oxide growth factor but also to the Pillings−Bedworth ratios of the elements and alloys.

Additionally fluoride species (due to their smaller ionic radius) usually show a faster migration rate than oxygen anions, and therefore accumulation at the metal oxide interface may be observed.[47] This fluoride layer than can remain present between cell boundaries and thus can act as a weak spot for stress and chemical dissolution induced separation. Such sensitized cell boundaries were observed in the case of pure Al.[6]

In summary, the present work investigates the self-ordering and morphological thresholds (porous/tubular) for the intermetallic compounds $TiAl_3$, TiAl, Ti_3Al, and Ti in HF-containing H_2SO_4 electrolytes. For the investigated Ti−Al alloys the formation of self-organized oxide layers can be observed over a wide range of anodizing potentials (in particular, a range of potentials that is wider than for pure Ti). A morphological change in the self-organized structures depending on anodization voltage and on alloy composition is observed—the occurrence of these tube separation effects are ascribed to increased stress that occurs within the growing oxides due to increasing volume expansion when altering the composition from Al toward Ti. This separation may be supported by sensitization of the cell boundaries by fluoride species. The correlation length of self-organization is found to be very well consistent with a semispherical oxidation model of Yasuda,[42] independent of whether tubular or porous morphology is formed.

Acknowledgment. The authors would like to acknowledge A. Friedrich and H. Hildebrand for SEM investigations and Deutsche Forschungsgemeinschaft (DFG) for financial support. Dr. M. Oehring at GKSS Forschungszentrum Geesthacht is gratefully acknowledged for providing the TiAl intermetallic compounds.

Supporting Information Available: Detailed experimental section and SEM images of cross sections, layers grown in HF free electrolytes, and current density transients of the investigated materials during anodization (PDF). This material is available free of charge via the Internet at http://pubs.acs.org.

CM8004024

(40) Ono, S.; Saito, M.; Ishiguro, M.; Asoh, H. *J. Electrochem. Soc.* **2004**, *151*, B473.
(41) Macak, J. M.; Tsuchiya, H.; Taveira, L.; Aldabergerova, S.; Schmuki, P. *Angew. Chem., Int. Ed.* **2005**, *44* (45), 7463.
(42) Yasuda, K.; Macak, J. M.; Berger, S.; Ghicov, A.; Schmuki, P. *J. Electrochem. Soc.* **2007**, *154* (9), C472.
(43) Skeldon, P.; Shimizu, K.; Thompson, G. E.; Wood, G. C. *Surf. Interface Anal.* **1983**, *5* (6), 247.
(44) Pillings, N. B.; Bedworth, R. E. *J. Inst. Metals* **1923**, *29*, 529.
(45) Nelson, J. C.; Oriani, R. A. *Corros. Sci.* **1993**, *34* (2), 307.
(46) Pringle, J. P. S. *Electrochim. Acta* **1980**, *25*, 1403.
(47) Habazaki, H.; Fushimi, K.; Shimizu, K.; Skeldon, P.; Thompson, G. E. *Electrochem. Commun.* **2007**, *9* (5), 1222.